ASE 4343 Project 1: Shockwave Analysis

Onitiana Razafimino[1]
Mississippi State University, Starkville, Mississippi, 39759, United States

The Schlieren images obtained experimentally have been run on ANSYS Fluent throughout this project. A personal interpretation of the results have also been provided in this report.

I. Nomenclature

β	=	Shockwave angle
CFD	=	Computational Fluid Dynamics
M_1	=	Upstream Mach number
M_2	=	Downstream Mach number
θ	=	Flow angle

II. Introduction

Schlieren photography is a technique used to observe a shock wave. By utilizing a special property of light which is the change of speed in a different medium, the variation of supersonic flows across a shockwave can be visualized. The denser is the medium, the slower is the light passing through it. The images from this experiment have been obtained, and a CFD analysis of each of the cases has been run on ANSYS. The formulas used are the ones used in class to analyze the properties of an oblique shockwave.

III. Methodology

A. Analytical methodology

Given the upstream Mach number M_1 and the shape angle θ, it is possible to predict M_2 and the shock angle β using the relation $\cot\theta = \tan\beta[\frac{(\gamma+1){M_1}^2}{2({M_1}^2 sin^2\,\beta-1)} - 1]$. To make calculations easy, the Compressible Aerodynamics Calculator offered online by Virginia Tech has been used to determine M_2 and β. Using Excel, a graph was drawn with β on the y-axis and θ on the x-axis for each Mach number to obtain the θ-β-M diagram.

B. Experimental methodology

Images from the Schlieren system have been provided. On these images, the angle θ and angle β can be measured. The Schlieren system utilizes the properties of fluctuations in density across the test section. While the fluid is tested and shockwaves are formed, the Schlieren system allows the visualization of those shock waves: when the air is less dense, the light travels slower. Light travels at different speeds across the shockwave, therefore an image showing a shockwave can be obtained. Using a protractor placed at the tip of the wedge on the image, the angle β is measured using a computer, as shown in Figure 1.

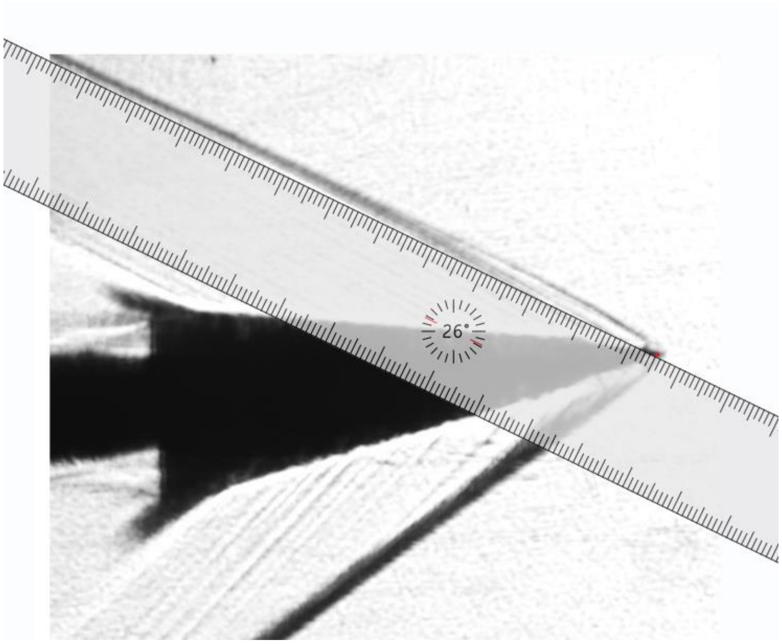

Figure 1: Image representing the method used to measure β

Once the angle β is obtained, the python script attached in the appendix is used to determine the Mach number M_2.

C. Computational methodology

The software ANSYS Fluent has been used to simulate the flow over the different wedges. Speos has been used to create a geometry and to generate a surface. As shown in figure 2, farfield 1 and farfield 2 are respectively 1.3m and 1.5m of length. The symmetry edge is 0.5m and the farfield 3 length will depend on the flow angle θ.

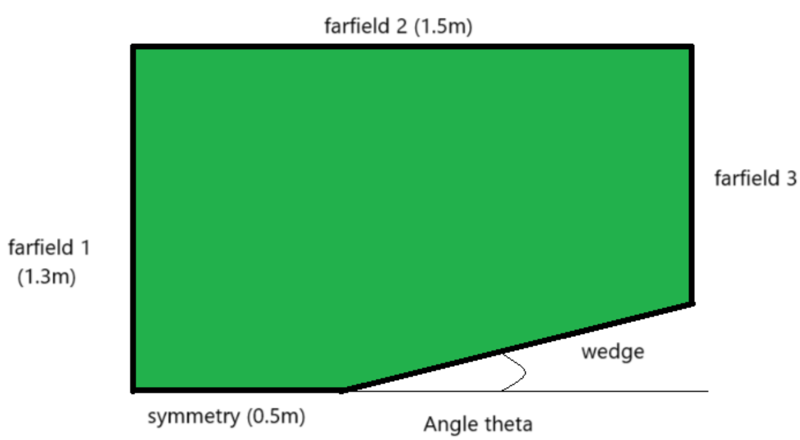

Figure 2: Dimensions of the surface generated in Speos.

Once the geometry is generated, the flow is run through Fluent, with a chosen Mach number and atmospheric conditions. The grid that is generated from the mesh is improved after a first series of simulations. The mesh is adapted, and using the gradient of static pressure, the mesh is refined. A refined mesh will be generated where the static pressure is varying. As expected, the mesh changed along the shock angle. As a result, the contour images become crispier. The grids can be found in Appendix A. Finally, to determine the shockwave angle, a curve has been generated along the shockwave, and the tangent of its slope corresponds to the shockwave angle.

IV. Results and Discussion

The *θ-β-M diagrams* of the analytical results and the computational results are very similar. They are almost coincident. The higher the Mach number is, the lower β is. This applies to all 3 cases. This is true because the faster the flow is, the more effectively it can be compressed. However, the three graphs differ in terms of the accuracy of the values of β. As an example, at Mach 2 and for θ = 15 deg., the analytical value of β is 45.34 deg., the experimental value of β is 44 deg., and the computational value of β is 45 deg. There is not much of a difference, but the gap can mean something experimentally.

First, to determine the accuracy of the computational results, figure 4 compares the values of β obtained analytically and computationally. The absolute values of error percentage vary from 0.076% to 3.07%, which is pretty good. Similarly, figure 5 compares the values of M_2 obtained analytically and computationally. In this case, the absolute values of error percentage vary from 0% to 0.222%, which is even better.

The higher percentage of error in the case of the angle β may be due to the method used to measure the angle. The endpoints used to draw the shockwave line have been placed visually on the contour. The value of Mach number M_2 and its very small deviation from analytical results means that the computational model can be trusted.

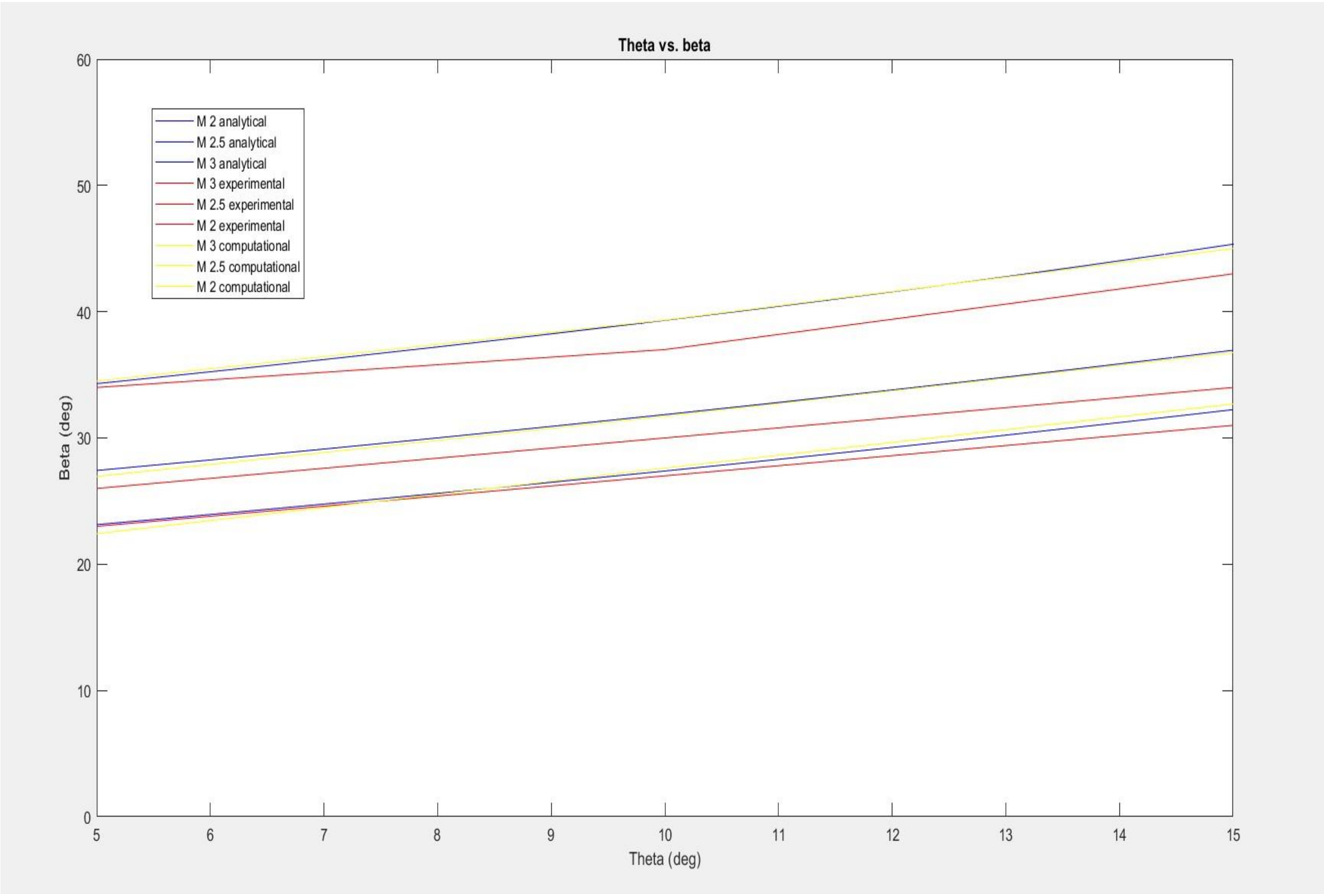

Figure 3: θ-β-M plot of analytical, experimental, and computational results. Blue represents the analytical results. Red represents the analytical results and yellow represents the computational results.

Mach number	θ (deg)	β analytical	β computational	%error
3	5	23.13	22.42	-3.07
	10	27.38	27.61	0.84
	15	32.24	32.69	1.40
2.5	5	27.42	26.95	-1.70
	10	31.85	31.72	-0.410
	15	36.94	36.76	0.490
2	5	34.30	34.51	0.612
	10	39.31	39.34	0.0760
	15	45.34	45	-0.750

Figure 4: Table representing the error percentages of β between analytical and computational results

Mach number	θ (deg)	M_2 analytical	M_2 computational	%error
3	5	2.75	2.75	0.00
	10	2.51	2.51	0.00
	15	2.255	2.25	-0.222
2.5	5	2.29	2.29	0.00
	10	2.09	2.09	0.00
	15	1.874	1.87	-0.213
2	5	1.822	1.82	0.110
	10	1.641	1.64	-0.0609
	15	1.446	1.44	-0.00415

Figure 5: Table representing the error percentages of M_2 between analytical and computational results

As it can be seen in the next two tables, the experimental errors are far higher than the computational errors. According to figure 6, they range from 0.562% to 7.96% for β. One thing to note is that the values of β recorded experimentally all have two significant digits. This is due to the quality and accuracy of the images provided. In some of these images, the shockwave line can be so thick that it becomes difficult to measure its angle. Also, the degree of accuracy of the tool chosen is in the order of degree.

Furthermore, according to figure 7, the experimental error for M_2 ranges from 1.20% to 21.40%. The wrong reading of β clearly results in the deviation of experimental Mach number to its analytical value. The error is propagated because the formula used to calculate Mach number is a function of β.

Mach number	θ (deg)	β analytical	β experimental	%error
3	5	23.13	23	-0.562
	10	27.38	27	-1.39
	15	32.24	31	-3.85
2.5	5	27.42	26	-5.18
	10	31.85	30	-5.81
	15	36.94	34	-7.96
2	5	34.30	34	-0.875
	10	39.31	38	-3.33
	15	45.34	44	-2.96

Figure 6: Table representing the error percentages of β between analytical and experimental results

Mach number	θ (deg)	M_2 analytical	M_2 experimental	%error
3	5	2.75	2.783	1.20
	10	2.51	2.587	3.07
	15	2.255	2.488	10.33
2.5	5	2.29	2.553	11.48
	10	2.09	2.376	13.68
	15	1.874	2.275	21.40
2	5	1.822	1.852	1.65
	10	1.641	1.754	6.89
	15	1.446	1.535	6.15

Figure 7: Table representing the error percentages of M_2 between analytical and experimental results

If the above interpretations are put together, it can be concluded that the experimental values of the angle β are slightly lower than the computational and the analytical values. Indeed, according to the θ-β-M diagram in figure 1, the three experimental curves are below the analytical and computational curves. This, in turn, results in a higher Mach number behind the shock wave. Indeed, according to figure 5, the percentage of errors are all positive.

This large gap may be due to the fact that, in the Schlieren optical system, the knife edge has some sort of volume. It is therefore a 3D object. In the theoretical analysis and computational analysis, the objects are both considered to be in 2 dimensions. Furthermore, the flow in the Schlieren system is viscous and the knife exerts friction on the fluid, which alters the results. According to what we learned in class, a blunt body has a lower shock angle than a wedge. This is exactly what is happening here.

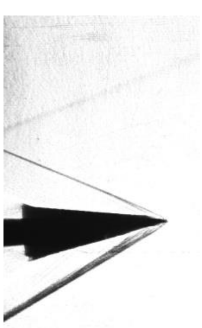

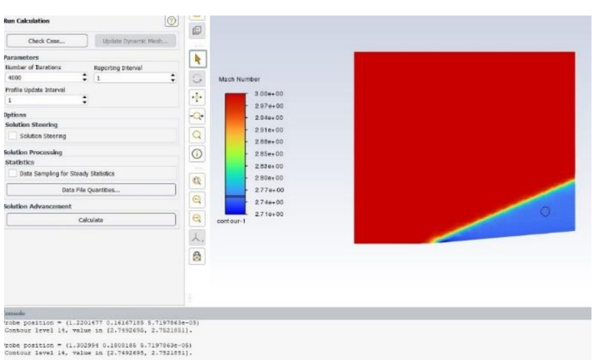

Figure 8: Schlieren image and CFD image of a Mach 3 flow at a 5 degrees wedge

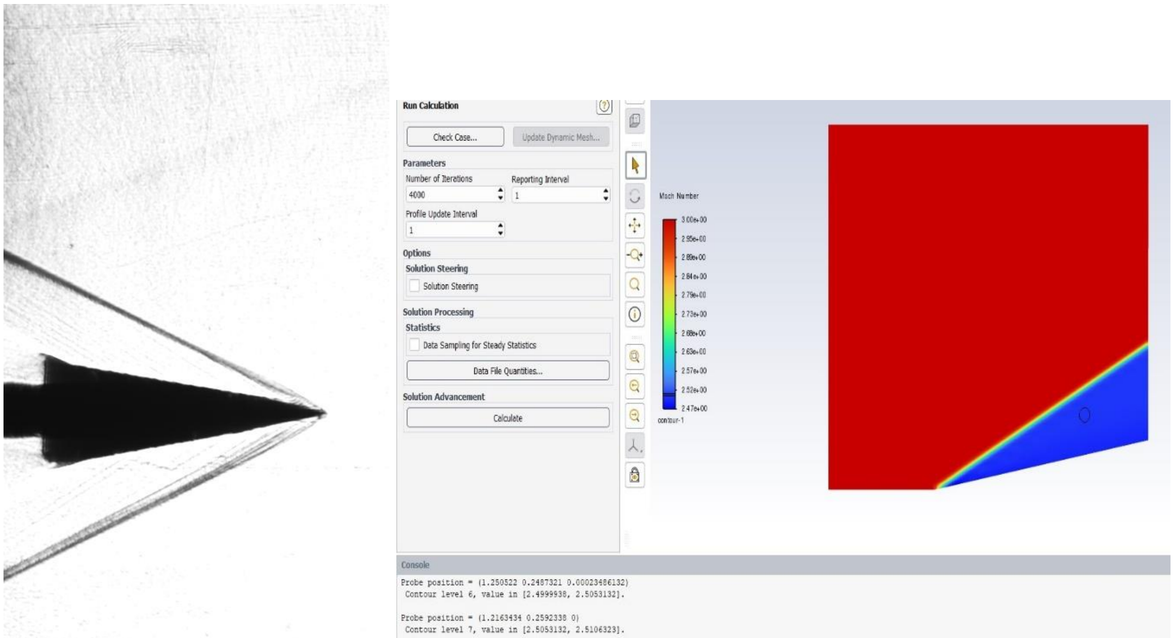

Figure 9: Schlieren image and CFD image of a Mach 3 flow at a 10 degrees wedge

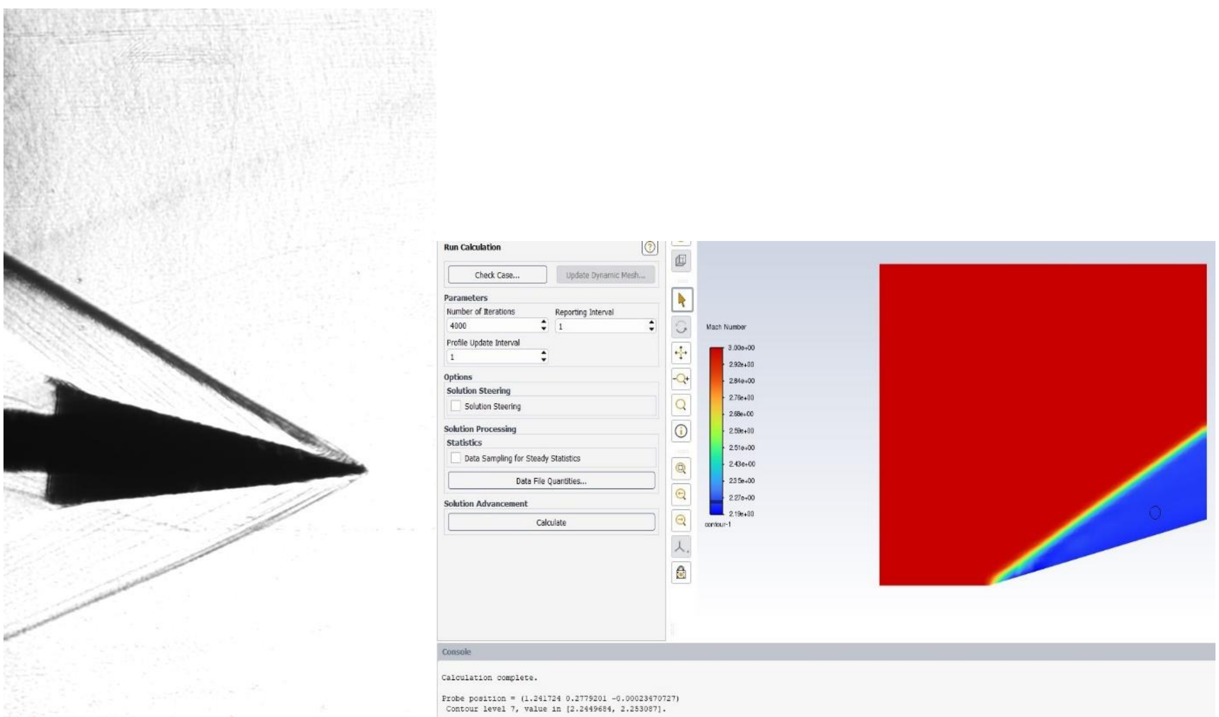

Figure 10: Schlieren image and CFD image of a Mach 3 flow at a 15 degrees wedge

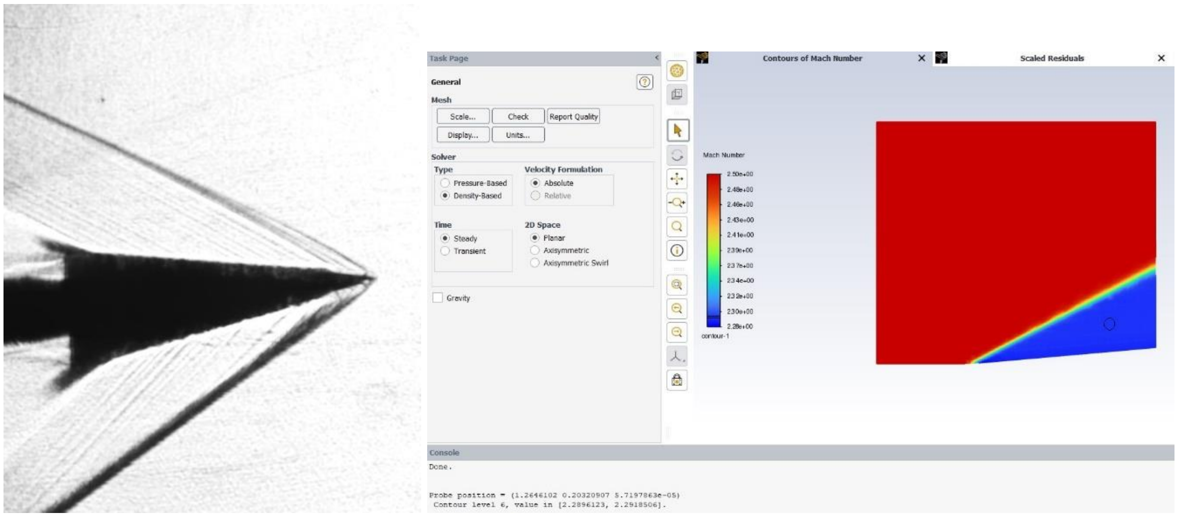

Figure 11: Schlieren image and CFD image of a Mach 2.5 flow at a 5 degrees wedge

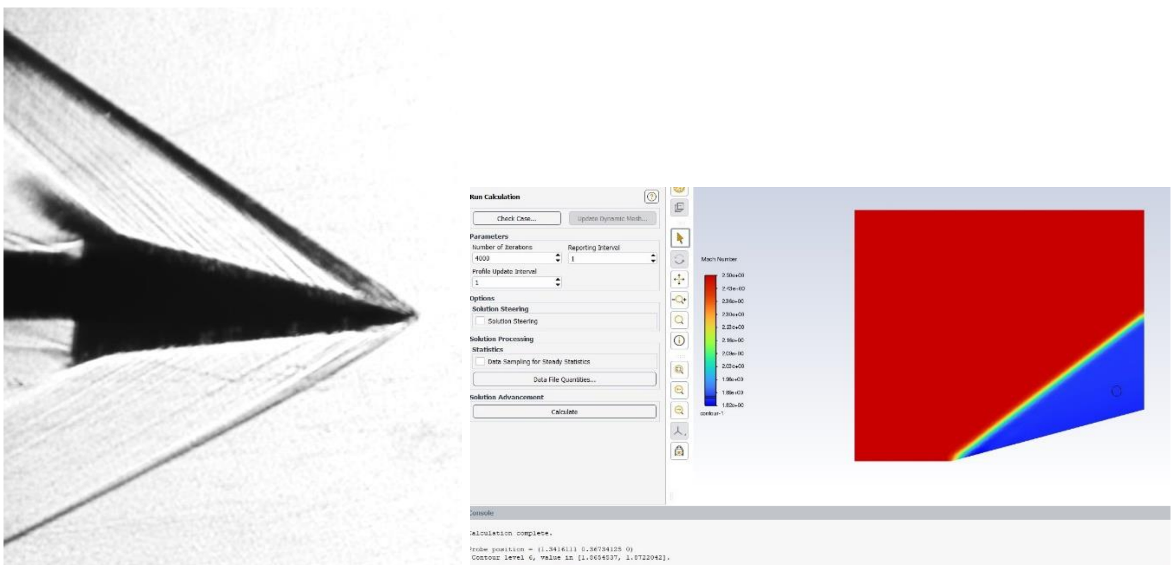

Figure 12: Schlieren image and CFD image of a Mach 2.5 flow at a 15 degrees wedge

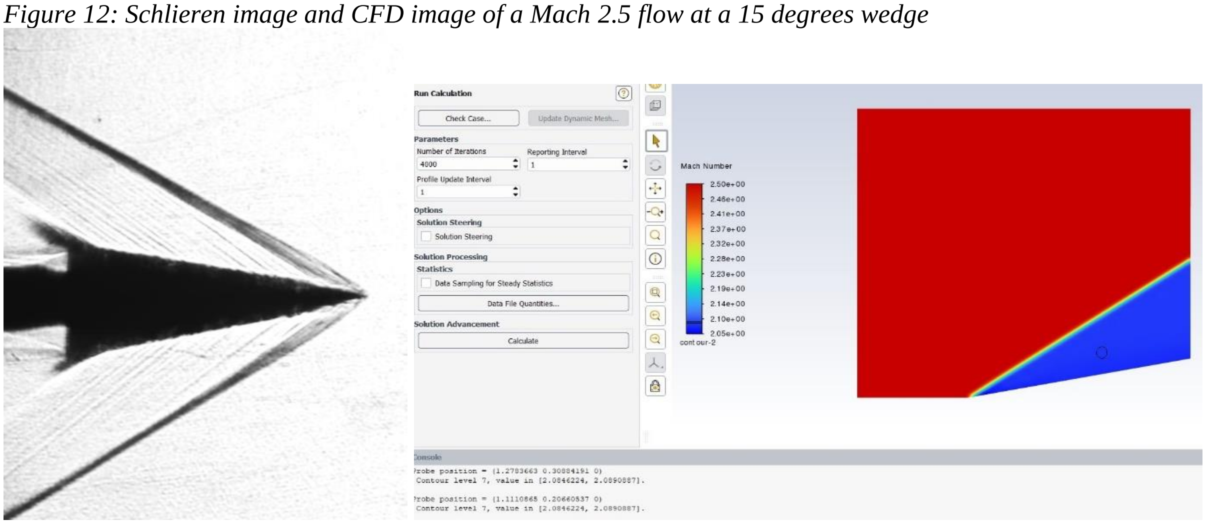

Figure 10: Schlieren image and CFD image of a Mach 2.5 flow at a 10 degrees wedge

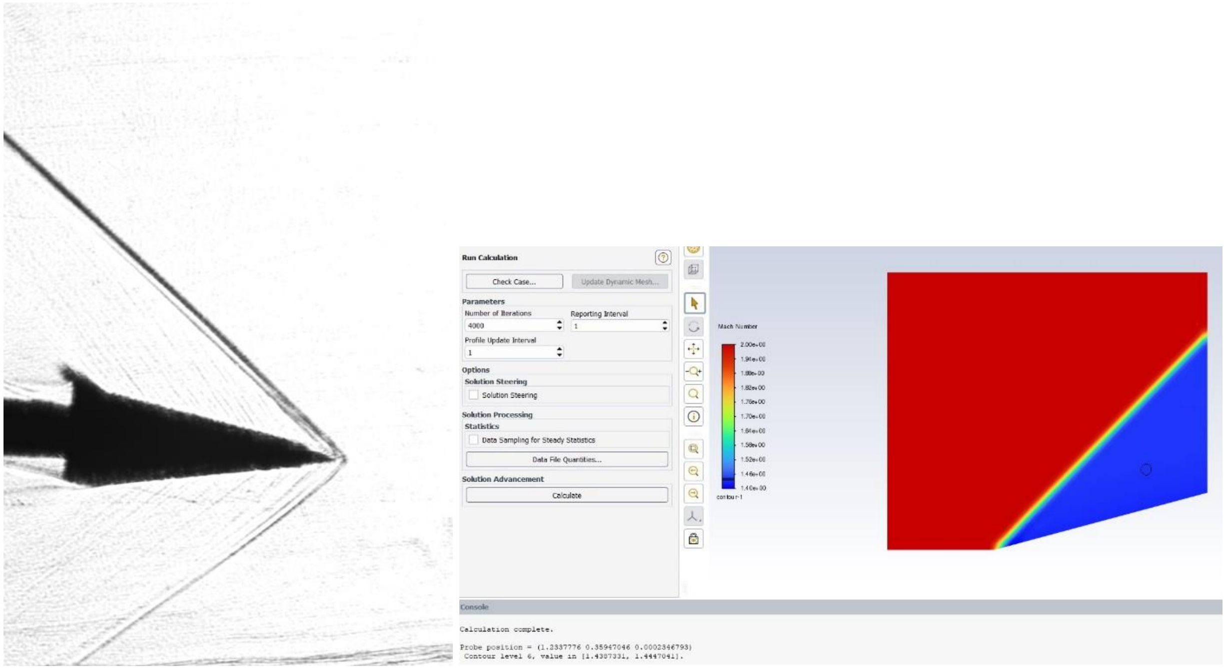

Figure 10: Schlieren image and CFD image of a Mach 2 flow at a 15 degrees wedge

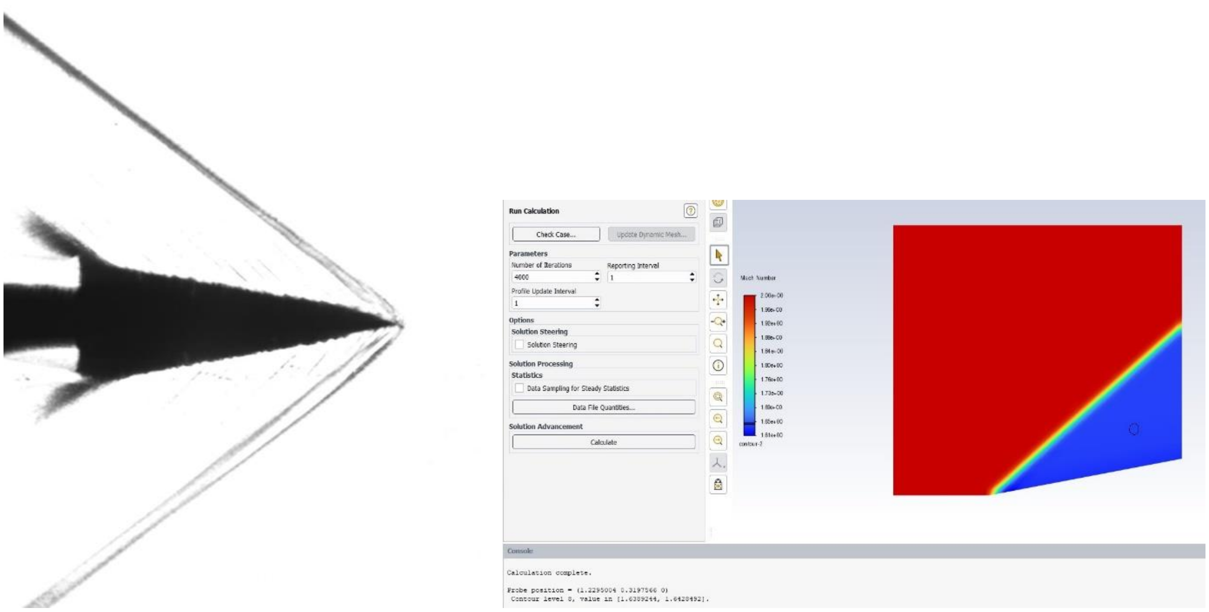

Figure 10: Schlieren image and CFD image of a Mach 2 flow at a 10 degrees wedge

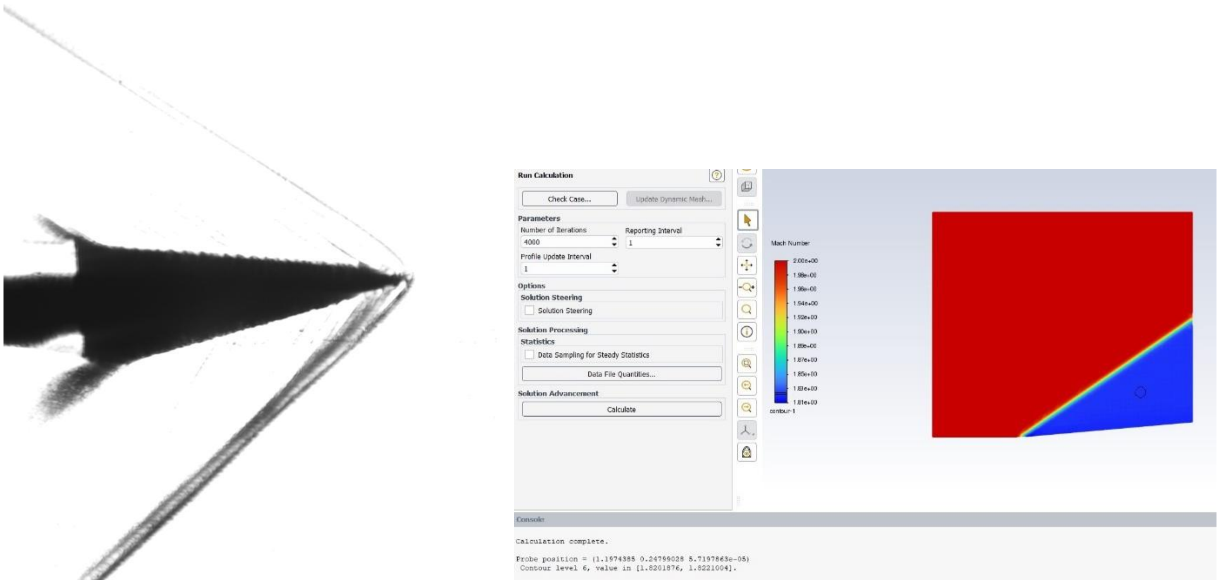

Figure 10: Schlieren image and CFD image of a Mach 2 flow at a 5 degrees wedge

It can be seen that the shockwave is thick very thick in all of the experimental cases. In some cases, the lines formed by the shockwave are crossing each other. The reason being is that a 3-dimensional object will have its shockwave surrounding the object. As stated before, theoretically, a blunt body results in a lower shock angle. There are also slight variations of Mach number along the edge. Indeed, some black lines are visible along the edge in the Schlieren images, like the case of a Mach 2.5 flow at a wedge angle of 5 degrees (figure 11). Those characteristics make the flow a little bit complicated to predict. On the other hand, there is no variation in Mach number in the 2-D case, which is the computational method, along the edge: the only color present along the edge is blue, which represents a uniform velocity.

Another limitation to the technique used in the experiment is the use of a protractor. Not knowing what the actual edge of the shockwave is is misleading, and the misreading of the angle, even by one degree, can alter the results.

V. Conclusion

It has been seen throughout this project that running computational simulations is important to validate data obtained from the experiment. However, computational modeling is not always the best representation of the actual experiment. In our case, even if the thickness of the knife edge is small, it can still change the results. No matter how small that thickness is, the knife is considered a three-dimensional object in a supersonic flow. It has been seen throughout the semester that there is a very important distinction between 3-dimensions and 2-dimensions. 3-dimensions cases are very difficult to model and sometimes do not have an analytical solution. Viscosity also needs to be taken into account. Before running computations and jumping to conclusions, the experiment variables must be considered and computational methods need to be thought through. Sometimes, inaccuracy can be acceptable. In our case, the Schlieren method is not recommended to calculate numerical results. It is a technique only used to "visualize changes or uniformities" (Mazumdar).

Appendix A: Table representing the analytical, experimental, and computational results

M_1	θ (deg)	β (deg)	M_2
3	5 10 15	23.13 27.38 32.24	2.75 2.51 2.255
2.5	5 10 15	27.42 31.85 36.94	2.29 2.09 1.874
2	5 10 15	34.30 39.31 45.34	1.822 1.641 1.446

Table representing Analytical results

Mach number	θ (deg)	Β (deg)	M_2
3	5 10 15	23 27 31	2.783 2.587 2.488
2.5	5 10 15	26 30 34	2.553 2.376 2.275

2	5 10 15	34 37 43	1.852 1.754 1.535

Table representing experimental results

Mach number	θ (deg)	B (deg)	M_2
3	5 10 15	22.42 27.61 32.69	2.75 2.51 2.25
2.5	5 10 15	26.95 31.72 36.76	2.29 2.09 1.87
2	5 10 15	34.51 39.34 45	1.82 1.64 1.44

Table representing the computational results

Appendix B: Grids used

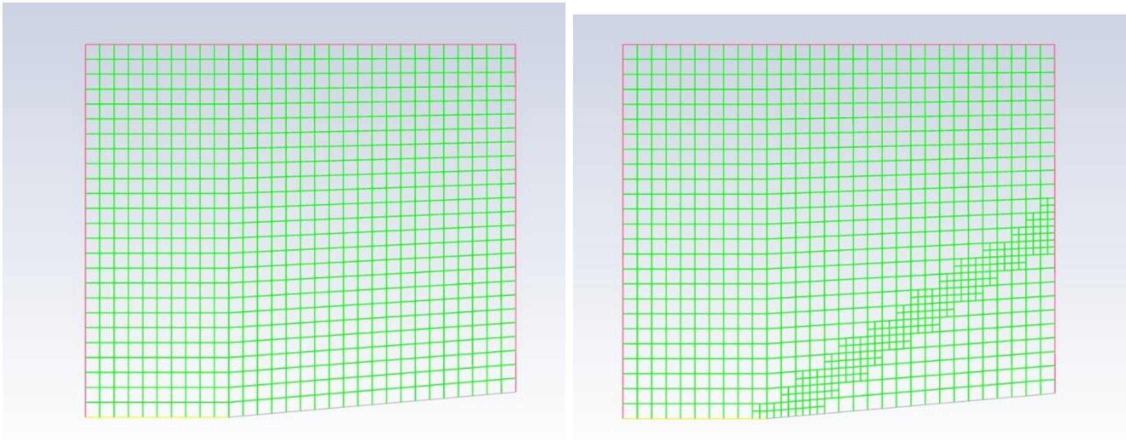

Grid Mach 2, 5 deg
Before: 750 meshes, After refinement: 921 meshes

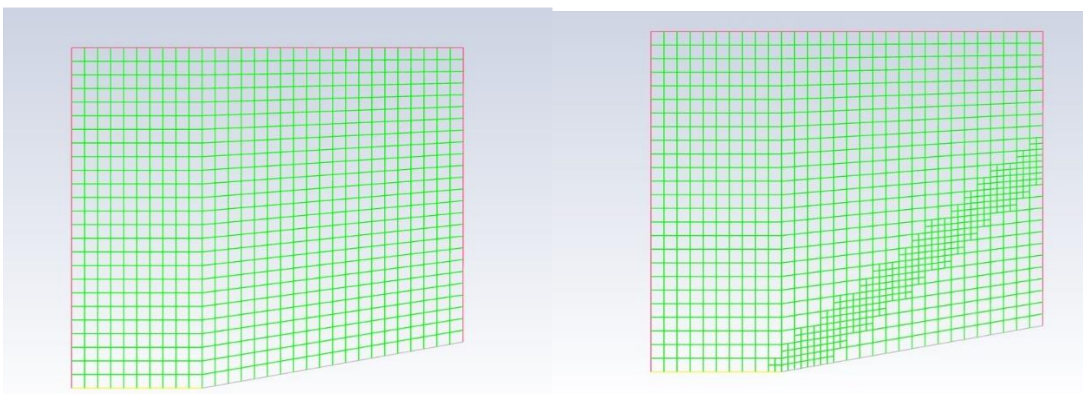

Grid for Mach 2, 10 deg
Before: 750 meshes, After refinement: 975 meshes

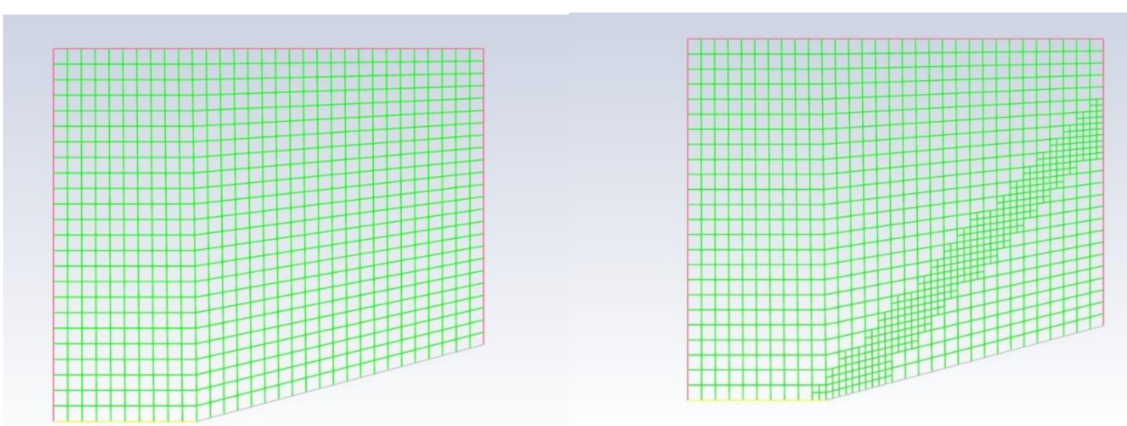

Grid for Mach 2, 15 deg

Before: 744 meshes, After adaptation: 996 meshes

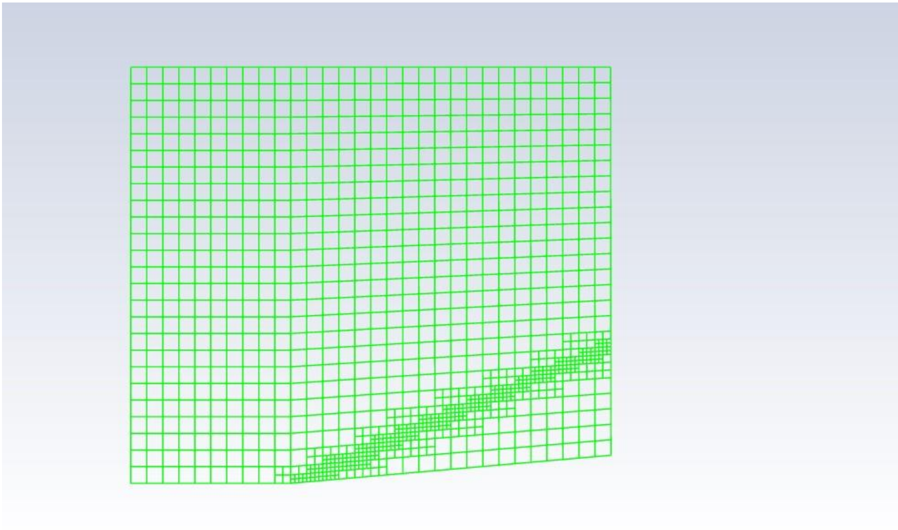

Grid for Mach 3, 5 deg

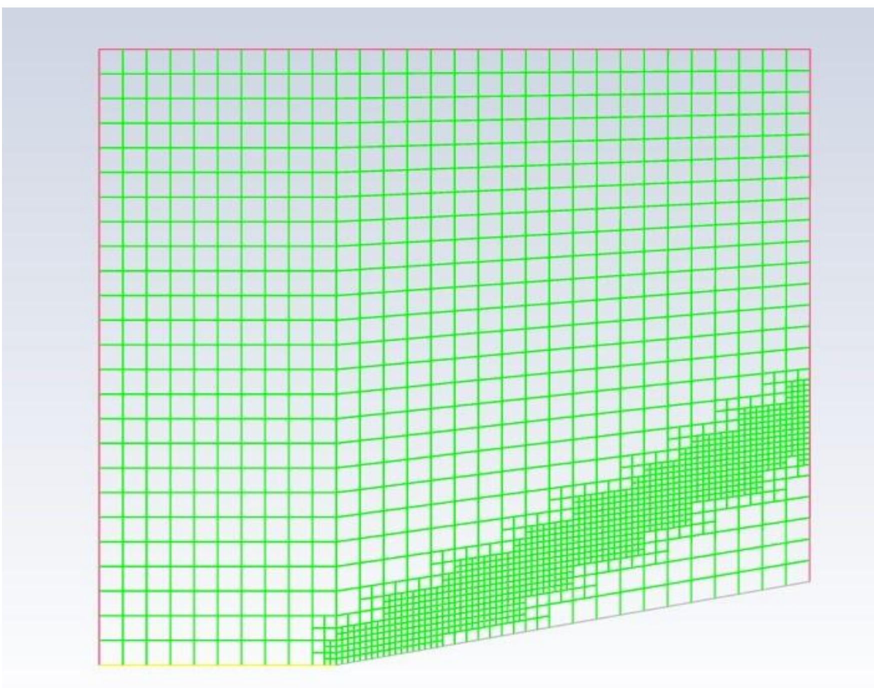

Grid for Mach 3, 10 deg

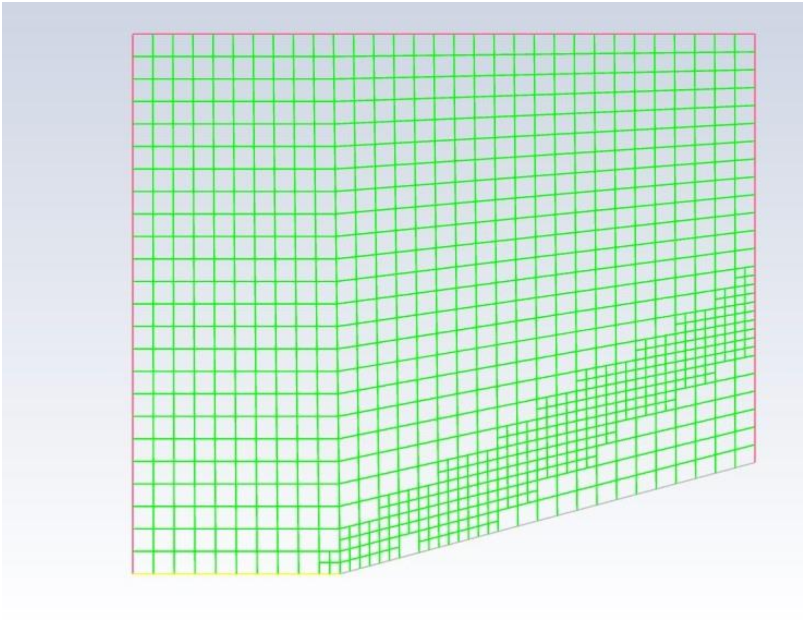

Grid Mach 3, 15 deg

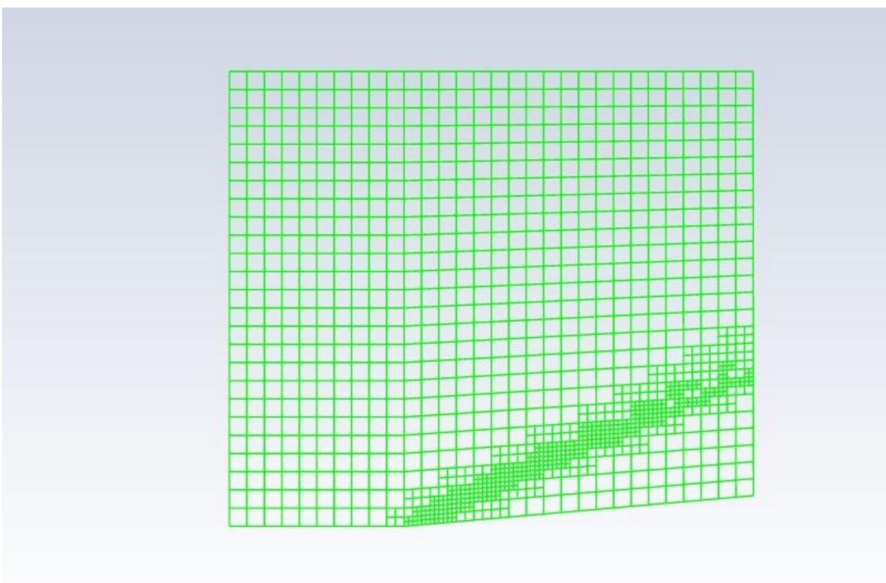

Grid for Mach 2.5, 5 deg

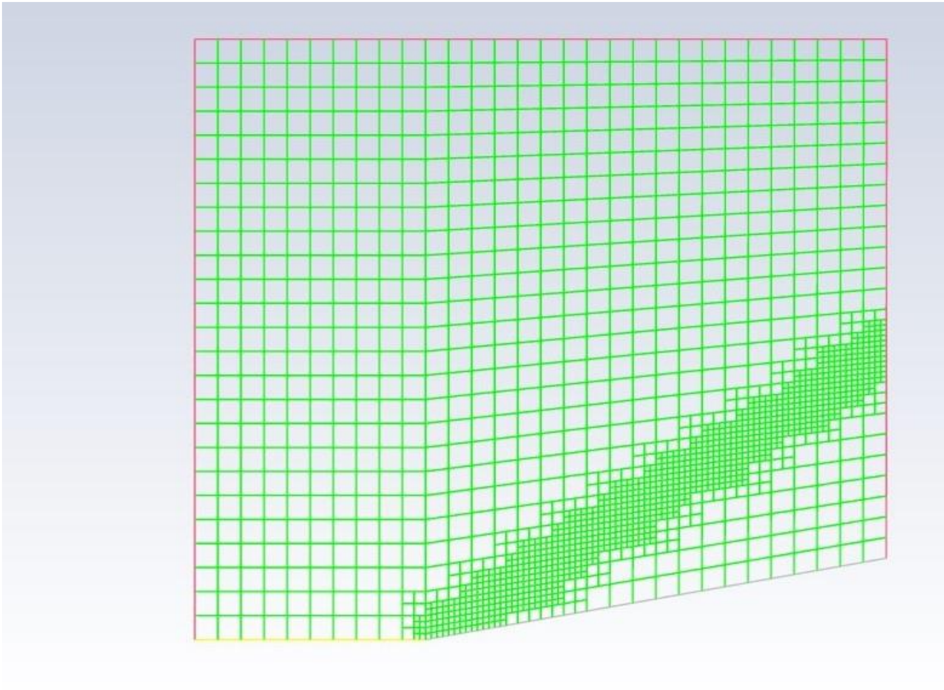

Grid for Mach 2.5, 10 deg

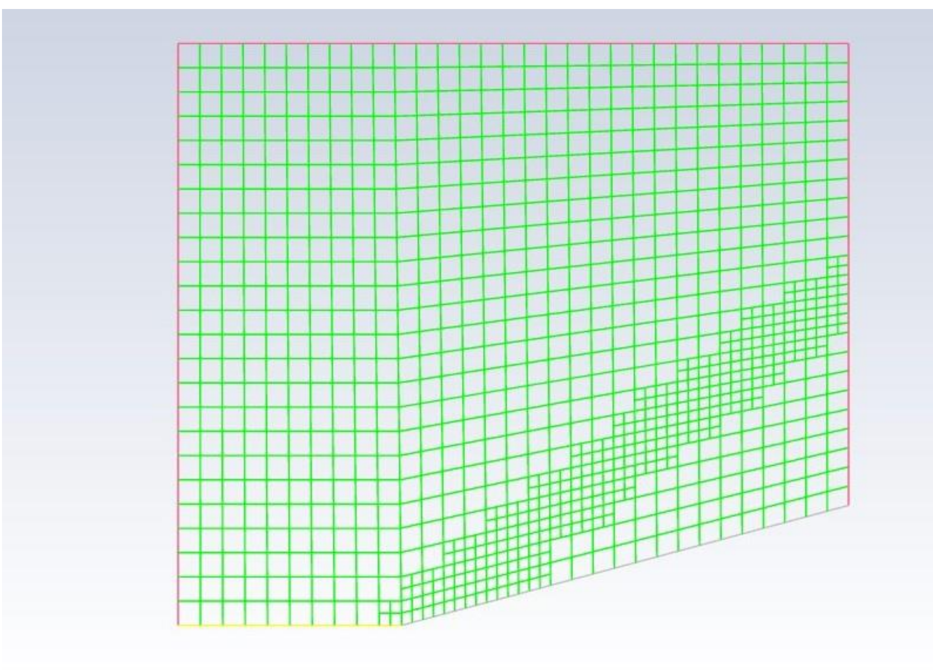

Grid for Mach 2.5, 15 deg

Appendix C: MATLAB Code used to produce the graph

```
gamma = 1.4;
Ma = 2;
Mb = 2.5;
Mc = 3;
beta = linspace(0, pi/2);
theta = acot(tan(beta).*((gamma+1)*Ma*Ma./(2*(Ma*Ma.*sin(beta).*sin(beta)-1))-1));

figure
plot(rad2deg(theta), rad2deg(beta), 'b');

hold on;

theta2 = acot(tan(beta).*((gamma+1)*Mb*Mb./(2*(Mb*Mb.*sin(beta).*sin(beta)-1))-1));
plot(rad2deg(theta2), rad2deg(beta), 'b');
hold on;

theta3 = acot(tan(beta).*((gamma+1)*Mc*Mc./(2*(Mc*Mc.*sin(beta).*sin(beta)-1))-1));
plot(rad2deg(theta3), rad2deg(beta), 'b');


hold on;
%Experimental

theta4 = [5 10 15];
betae3 = [23*pi/180 27*pi/180 31*pi/180];
plot(theta4, rad2deg(betae3), 'r');
hold on
betae4 = [26*pi/180 30*pi/180 34*pi/180];
plot(theta4, rad2deg(betae4), 'r');

hold on
betae5 = [34*pi/180 37*pi/180 43*pi/180];
plot(theta4, rad2deg(betae5), 'r');
hold on
%Computational

theta4 = [5 10 15];
betac3 = [22.42*pi/180 27.61*pi/180 32.69*pi/180];
plot(theta4, rad2deg(betac3), 'y');
hold on
betac4 = [26.95*pi/180 31.72*pi/180 36.76*pi/180];
plot(theta4, rad2deg(betac4), 'y');

hold on
betac5 = [34.51*pi/180 39.34*pi/180 45*pi/180];
plot(theta4, rad2deg(betac5), 'y');
hold off



axis([rad2deg(5*pi/180) rad2deg(15*pi/180) 0 rad2deg(pi/3)]);
```

```
xlabel('Theta (deg)');
ylabel('Beta (deg)');
title('Theta vs. beta');


legend("M 2 analytical", "M 2.5 analytical", "M 3 analytical", ...
    "M 3 experimental", "M 2.5 experimental", "M 2 experimental", ...
    "M 3 computational", "M 2.5 computational", "M 2 computational");
```

References

[1] Ansys Inc. Workbench with Speos 2024 R1. Canonsburg, Pennsylvania

[2] Mathworks. MATLAB Version R2024B. Natick, Massachusetts

[3] Mazumdar, A. (2013, June 18). (PDF) study of Schlieren Optical visualization basics technique and the principle. https://www.researchgate.net/publication/276279333_Study_of_Schlieren_Optical_Visualization_Basics_Technique_and_the_Principle